Climate and Vegetation History of the Midcontinent from 75 to 25 ka: A Speleothem Record from Crevice Cave, Missouri, USA

Jeffrey A. Dorale,* R. Lawrence Edwards, Emi Ito, Luis A. González

Four Missouri stalagmites yield consistent overlapping records of oxygen and carbon isotopic changes and provide a climate and vegetation history with submillennial resolution from 75 to 25 thousand years ago (ka). The thorium-230–dated records reveal that between 75 and 55 ka, the midcontinental climate oscillated on millennial time scales between cold and warm, and vegetation alternated among forest, savanna, and prairie. Temperatures were highest and prairie vegetation peaked between 59 and 55 ka. Climate cooled and forest replaced grassland at 55 ka, when global ice sheets began to build during the early part of Marine Oxygen Isotope Stage 3.

Records of midcontinental climatic conditions throughout early parts of the last glacial period are scarce, and of these, dating has been problematic but is needed to allow meaningful comparison with the marine record of global climatic changes. Much of this period is beyond reliable radiocarbon control, which extends back to only 40 to 45 ka. We applied high-precision ^{234}U-^{230}Th dating to the $\delta^{13}C$ and $\delta^{18}O$ profiles of four calcite stalagmites from Crevice Cave, southeastern Missouri, USA (37°45′N, 89°50′W) (Fig. 1). The ^{234}U-^{230}Th chronometer extends the datable range to 500 ka (*1*) and has been successfully applied to corals (*2*) and inorganic calcite precipitates such as groundwater veins (*3*) and speleothems (*4*). Crevice Cave lies near the present-day ecotone between deciduous forest and tall-grass prairie and is sensitive to climatic change. The site is ideal for recording glacial-age climate, because Laurentide ice lobes advanced to within several hundred kilometers of the cave during the last glacial period.

Crevice Cave is Missouri's longest known cave and contains more than 45 km of mapped passages. The stalagmites we studied were found naturally broken within a stream-level passage approximately 25 m below the ground surface. The four stalagmites, labeled CC\DBL-L, CC\DBL-S, CC\C, and CC\E, were separated from one another by 100 to 200 m and were located approximately 1 km from the nearest known entrance (*5*). When split and polished, stalagmites appeared pristine and gave no indication of postformational alteration.

We milled powders for $\delta^{13}C$ and $\delta^{18}O$ analysis (*6*) with a 0.5-mm dental burr at a sampling interval of 1 to 3 mm along the central growth axis of each stalagmite. Sample sizes for U-Th analysis were 150 to 300 mg, so that the number of years averaged in a sample approached that of the U-Th analytical error (100 to 300 years) (*7*). We obtained 38 U-Th analyses for the four stalagmites, using thermal ionization mass spectrometry (Table 1) (*8*). For each stalagmite, all ages are in correct stratigraphic order, suggesting that these dense calcite stalagmites have remained closed to U and Th migration and that our age determinations are accurate. Ages for $\delta^{13}C$ and $\delta^{18}O$ values are assigned by linear interpolation between dated intervals (*9*).

Values of $\delta^{13}C$ for the Crevice Cave stalagmites vary from –9.7 to –1.8 per mil (Fig. 2). Despite differences in growth rate, color, banding features, and trace-element concentrations among the four stalagmites, trends in $\delta^{13}C$ values are similar and imply that different hydrologic characteristics between specific drip pathways (*10*) cannot account for the long-term changes in speleothem $\delta^{13}C$ values. Instead, these trends likely reflect a more pervasive influence, such as the changing $\delta^{13}C$ composition of the overlying soil and vegetation.

Speleothem $\delta^{13}C$ values are linked to vegetation because cave drip waters first pass through the overlying soil, and soil organic matter is derived from vegetation. Large variations in soil organic matter $\delta^{13}C$ values result from differences between the C_3 and C_4 photosynthetic pathways; C_3 plants have $\delta^{13}C$ values from –32 to –22 per mil, averaging ~–27 per mil, whereas C_4 plants have values from –16 to –9 per mil, averaging ~–12 per mil (*11*). C_4 plants are typically warm-season grasses found in tropical and temperate grasslands, whereas C_3 plants are mostly trees, cool-season grasses, and forbs. Although $\delta^{13}C$ values are modified as infiltrating water dissolves carbonate bedrock enroute to underlying caves (*12*), the relative contribution of C_3 and C_4 plants is maintained. Preserved $\delta^{13}C$ signatures may thus serve as indicators of the prevalence of forests versus grasslands through time.

This relationship between vegetation type and speleothem $\delta^{13}C$ values has been confirmed and calibrated in a number of studies on well-dated Holocene speleothem, pollen, plant-macrofossil, and sedimentary organic matter sequences from northeast Iowa (*13*). At Cold Water Cave, stalagmite $\delta^{13}C$ values varied from –9.1 to –4.2 per mil and tracked (for several thousand years) the $\delta^{13}C$ values of nearby sedimentary organic matter as well as transitions from deciduous forest to prairie to oak savanna, as revealed in nearby alluvial deposits at Roberts Creek. These high-resolution studies also revealed that rapid, decade-scale transitions in vegetation initiate gradual, millennial-scale turnover of the soil organic matter, at least for the deep soils of Iowa.

Sediment records from small basin lakes in south-central Illinois (*14*) are less than 200 km from Crevice Cave and provide the best opportunity for a midcontinental, pollen-based vegetation history during the early Wisconsinan glacial period. These basins formed as kettles during late-Illinoian time (~140 ka) and escaped obliteration because of less extensive Wisconsinan ice. The pollen records (*14, 15*) show marked variations from conifer to temperate forest, with prominent intervals of prairie or prairie/forest border vegetation (*16*). Thus, these records document conspicuous vegetation and climate changes in the midcontinent during the Wisconsinan period, but the timing is poorly known because of the inability to date these types of sediments precisely and accurately.

Our data show several oscillations in $\delta^{13}C$ values that we interpret as transitions between forest and grassland environments (Fig. 2). The issue of millennial-scale soil organic matter storage is important in these interpretations, because the storage phenomenon dampens the magnitude of initial speleothem $\delta^{13}C$ response to the actual vegetation change. Thus, the $\delta^{13}C$ trends are gradual, and the timing of the actual vegetation change is represented not necessarily by some instantaneous value of $\delta^{13}C$ but instead by a robust inflection in the $\delta^{13}C$ profile.

The most notable feature of the Crevice Cave vegetation history is that grassland-type

J. A. Dorale, R. L. Edwards, E. Ito, Department of Geology and Geophysics, University of Minnesota, Minneapolis, MN 55455, USA. L. A. González, Department of Geology, University of Iowa, Iowa City, IA 52242, USA.

*To whom correspondence should be addressed. E-mail: dora0011@tc.umn.edu

environments dominated between 71 and 55 ka, during Marine Oxygen Isotope Stage 4 and the early part of Stage 3, and that forest persisted from 55 to 25 ka (*17*). Between 59 and 55 ka, high $\delta^{13}C$ values suggest that the cave region was a grassland of high C_4 plant biomass.

Whereas speleothem $\delta^{13}C$ is sensitive to vegetation conditions, $\delta^{18}O$ is linked to meteoric water. For the modern midlatitudes, the $\delta^{18}O$ value of mean annual precipitation (MAP) in continental interiors is observed to be largely a function of mean annual atmospheric temperature (MAT) (*18*). The modern empirical relation between MAP $\delta^{18}O$ values and MAT is about 0.6 per mil/°C. Other factors, however, may obscure this relation; precipitation derived from different air masses often has distinct $\delta^{18}O$ signatures, and seasonal variations in the $\delta^{18}O$ value of precipitation can be pronounced even when derived from a single air mass. Thus, any strict paleotemperature reconstruction must assume that neither the moisture source nor the seasonality of precipitation has varied significantly through time. Caves are well suited for such reconstructions, because ambient temperatures in poorly ventilated areas of deep caves (>11 m) are stable year-round and reflect the mean surface atmospheric temperature over several years (*19*).

Crevice Cave $\delta^{18}O$ values (Fig. 3) range from ~–3.6 to –5.0 per mil. Although many aspects of atmospheric circulation during the last glacial period remain unknown, we consider the simplest scenario in which this variation primarily reflects a change in MAT (*20*). In this scenario, the MAP $\delta^{18}O$–MAT relation of 0.6 per mil/°C is counteracted by the –0.26 per mil/°C fractionation between calcite and water (*21*) during crystallization, resulting in a net speleothem $\delta^{18}O$–MAT relationship of ~0.35 per mil/°C. Thus, the Crevice Cave $\delta^{18}O$ range of ~1.4 per mil represents a MAT range of approximately 4°C. The warmest temperatures were around 57 ka, and the coldest were at ~46 and 41 ka, culminating a cooling trend initiated at 55 ka.

Both the $\delta^{18}O$ and $\delta^{13}C$ records show a prominent event at 55 ka, indicating major climatic and environmental change. Age estimates for the basal Roxana Silt, a widespread loess blown from outwash plains of the first advance of Laurentide ice into the Upper Mississippi valley during the Wisconsinan glacial period (*22–24*), range from 45 to 55 ka (*25, 26*). Pedogenic features of the Roxana Silt imply that climatic conditions became cooler and less conducive to soil formation as deposition of the loess progressed (*24*). Spruce charcoal that occurs throughout much of the Roxana Silt in Wisconsin (*24*), along with pollen evidence from northern Illinois (*27*), suggest that the Upper Mississippi valley was dominated by a conifer forest during the period of Roxana Silt deposition. Farther south at Crevice Cave, the $\delta^{13}C$ values are also consistent with forest during this period.

The extreme conditions suggested by the Crevice Cave $\delta^{18}O$ record around 46 and 41 ka may be represented by a recently described till that lies below the well-studied Des Moines Lobe till, of 15 to 14 ka, in Iowa (*28*). Wood from this till yielded a single ^{14}C age of 41.8 ± 1.6 ka, hinting that a Laurentide ice lobe already occupied central Iowa before ~40 ka. Warmer climatic conditions eventually followed, as suggested by widespread evidence for episodes of rejuvenated soil-forming conditions throughout Illinois between ~37 and 25 ka (*23*). The Crevice Cave $\delta^{18}O$ record shows a jump at 37 ka to less-negative values and conditions that were approximately 2°C warmer.

Before 55 ka, climatic conditions appear to have oscillated more frequently. Several short-lived drops in $\delta^{18}O$ values culminate at ~74, ~71, and ~64 ka. These excursions represent cooling of about 2° to 3°C during Marine Oxygen Isotope Stage 4, a period of global ice buildup and presumably colder global temperatures (*29*). Instead of unidirectional cooling, the Crevice Cave $\delta^{18}O$ record suggests that the midcontinental climate was characterized by cool/warm oscillations every 3000 to 7000 years. This frequency resembles that of the glacial-period climatic oscillations observed in North Atlantic marine sediments and ice cores, most notably the Heinrich events and Dansgaard-Oeschger cycles (*30*).

The chronology of the Crevice Cave record raises several questions about midcontinental and global climatic changes. From ~59 to 55 ka, high $\delta^{13}C$ values suggest that the site was a grassland of high C_4 plant biomass, and the $\delta^{18}O$ values suggest that temperatures were warmest for the period from 75 to 25 ka. Although well-dated records for comparison are sparse, a British flowstone known to have grown during times of relative warmth during the last glacial cycle grew at 57.9 ± 1.5 ka (*31*), suggesting that the warm interval from 59 to 55 ka that we have identified in Missouri may have affected a broad area of the globe. Midcontinental warming from 59 to 55 ka also seems compatible with the marine record, because the transition from Marine Oxygen Isotope Stage 4 to Stage 3 at ~59 ka is marked by decreasing global ice volume (Fig. 3). Milankovitch forcing appears consistent with

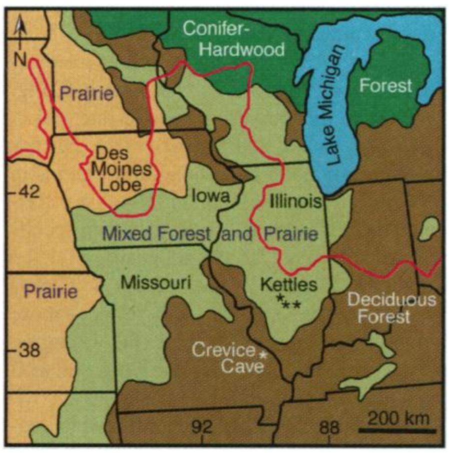

Fig. 1. Presettlement vegetation of the Midwest. Red line marks the maximum extent of Wisconsinan glaciation. Shown are the locations of Crevice Cave, pre-Wisconsinan kettle basins in Illinois, and the late-Wisconsinan (15 to 14 ka) Des Moines Lobe in Iowa.

Table 1. Thorium-230 ages of stalagmite subsamples. Distances are from the base of each stalagmite to the nearest half millimeter. Errors in age are 2σ and include analytical errors and uncertainties in initial $^{230}Th/^{232}Th$, propagated through the age equation. For the two subsamples with errors larger than a thousand years, the error is dominated by uncertainties in initial $^{230}Th/^{232}Th$. All other subsamples have corrections for initial ^{230}Th that are smaller than the analytical error. Half-lives are those used in (*2*). A full data table with isotope ratios and concentrations is available at the *Science* Web site (*8*).

Distance (mm)	Age and error (years)
	CC\DBL-L
252.5	26,930 ± 120
237.0	33,840 ± 140
216.0	40,310 ± 120
189.0	43,150 ± 220
161.0	48,270 ± 380
122.5	53,380 ± 270
116.0	54,780 ± 200
82.5	56,320 ± 250
65.0	58,040 ± 230
30.5	62,540 ± 700
8.5	65,580 ± 2,700
	CC\DBL-S
200.0	28,890 ± 160
194.0	31,500 ± 130
186.0	34,550 ± 120
183.0	35,650 ± 130
178.5	37,120 ± 180
173.0	39,240 ± 120
157.5	42,330 ± 130
84.0	54,780 ± 190
75.5	56,620 ± 250
9.0	64,670 ± 2,170
	CC\C2
203.5	21,940 ± 110
188.5	33,900 ± 720
185.0	38,450 ± 270
167.0	45,840 ± 510
161.5	49,510 ± 390
155.0	52,390 ± 330
145.0	55,810 ± 350
124.0	59,660 ± 240
98.0	65,070 ± 610
47.5	71,490 ± 760
8.0	74,060 ± 360
	CC\E1
106.5	35,710 ± 730
73.5	45,860 ± 190
61.5	54,510 ± 310
43.5	60,550 ± 320
25.0	65,490 ± 410
11.5	68,070 ± 640

the warming, because Northern Hemisphere summer insolation peaked around 58 ka (*32*).

The rapid climatic cooling at 55 ka in central North America is more difficult to explain. Laurentide ice advance into the Upper Midwest at 55 ka, as suggested by some age estimates for the basal Roxana Silt (*25*), actually seems an unlikely event considering that the marine $\delta^{18}O$ record suggests that global ice volume decreased from 61 to 55 ka. However, this scenario is complicated by uncertainties about the relationship between Laurentide and global ice volume, and Laurentide ice volume versus the frontal position of Laurentide ice. Taking the marine $\delta^{18}O$ chronology at face value, we note that the climatic change at 55 ka at Crevice Cave coincides with the onset of global ice buildup during Stage 3. Thus, global and midcontinental climate may have both cooled synchronously at 55 ka. Given the relatively warm conditions from 59 to 55 ka suggested by both the Crevice Cave and the marine records, we speculate that the spread of glaciation into the Upper Mississippi valley may have lagged behind the climatic cooling at 55 ka by several thousand years. We therefore suspect that the basal Roxana Silt age estimates of 55 ka are somewhat too old and that the estimates of 50 ka may be closer to the true age.

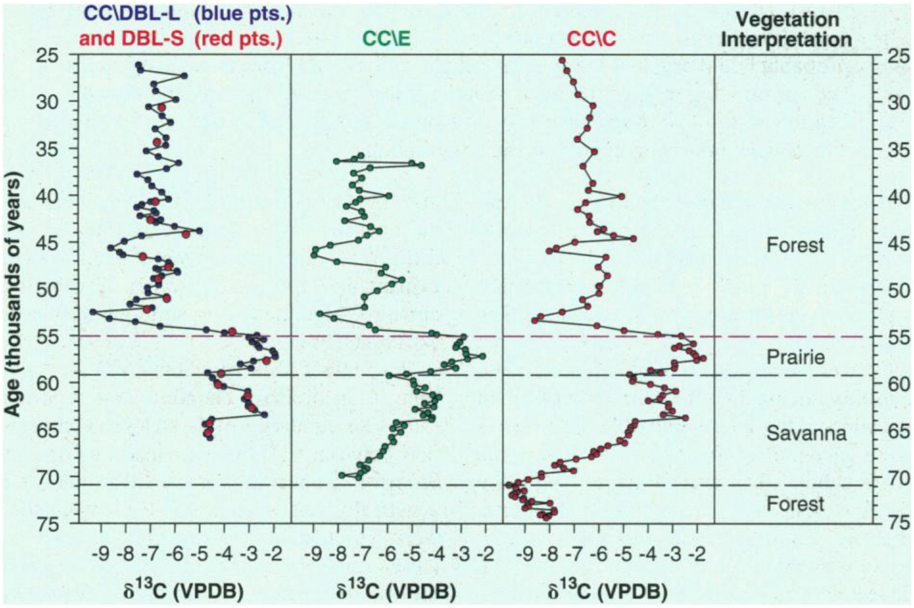

Fig. 2. Carbon isotope profiles for the Crevice Cave stalagmites and interpreted vegetation changes. The times of major vegetation transitions are highlighted by the dashed lines.

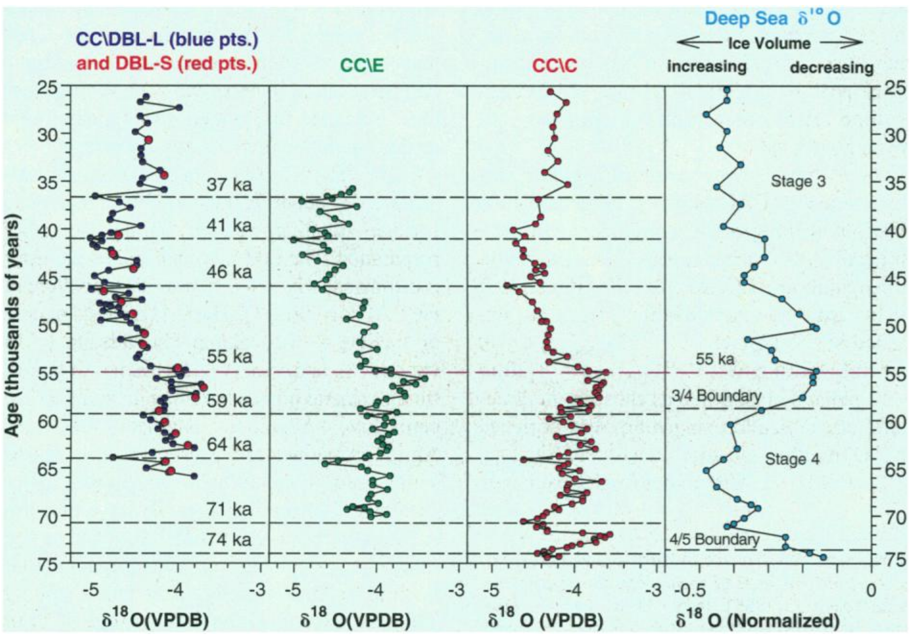

Fig. 3. Oxygen isotope profiles for the Crevice Cave stalagmites versus the normalized deep sea curve and chronology of Martinson *et al.* (*29*). Timing of key climatic events is highlighted by dashed lines.

References and Notes

1. R. L. Edwards, J. H. Chen, T.-L. Ku, G. J. Wasserburg, *Earth Planet. Sci. Lett.* **81**, 175 (1987).
2. R. L. Edwards *et al.*, *Science* **260**, 962 (1993).
3. I. J. Winograd *et al.*, *ibid.* **258**, 255 (1992).
4. R. S. Harmon, P. Thompson, H. P. Schwarcz, D. C. Ford, *Natl. Speleo. Soc. Bull.* **37**, 21 (1975); D. A. Richards, P. L. Smart, R. L. Edwards, *Nature* **367**, 357 (1994).
5. Stalagmites CC\DBL-L and CC\DBL-S grew side by side, separated by approximately 5 cm at their centers, and are joined together by coherent, traceable calcite growth.
6. Stable-isotopic analyses were made at two facilities: the Minnesota Isotope Lab and the University of Michigan Stable Isotope Lab, allowing interlaboratory comparison. Replication between labs was excellent. Values of $\delta^{13}C$ and $\delta^{18}O$ are reported relative to VPDB. Precision based on standard runs is better than ± 0.10 per mil.
7. Analytical procedures are similar to those in (*1*, *2*). Powdered samples were dissolved in 2 M HNO_3, spiked with a ^{229}Th-^{233}U-^{236}U tracer, coprecipitated with $FeOH_3$, and purified by anion-exchange chromatography. Samples were loaded onto rhenium ribbons in a double-filament configuration for U analysis and on single graphite-covered filaments for Th analysis. A Finnigan MAT 262-RPQ thermal ionization instrument with ion counting detection systems was used to determine U and Th concentrations and isotopic compositions. Reported age errors are based on the analytical precision; within-run statistics were comparable to counting statistics.
8. A full data table reporting ^{238}U and ^{232}Th concentrations, $^{230}Th/^{238}U$ ratios, and $\delta^{234}U$ values for each subsample is available as supplementary material at the *Science* Web site (www.sciencemag.org/feature/data/983892.shl).
9. Because growth rates vary (between 0.8 to 15.4 mm per 1000 years), some error is introduced by interpolation, but the high density of dates ensures that this error is small. However, interpolation and differential growth rates may account for the occasional small offsets between the four stable-isotope records. The largest errors most likely are from 40 to 25 ka, the interval where growth rates and thus sampling densities are lowest. Because of different growth rates for each stalagmite, before 55 ka CC\C and CC\DBL-L provide maximum resolution and accuracy, and after 55 ka CC\DBL-L provides the best chronological control.
10. A. Baker, E. Ito, P. L. Smart, R. F. McEwan, *Chem. Geol.* **136**, 263 (1997).
11. L. L. Tieszen and T. Boutton, in *Stable Isotopes in Ecological Research*, P. W. Rundel, J. R. Ehlerlinger, K. A. Nagy, Eds. (Springer-Verlag, New York, 1989), pp. 167–195.
12. Elevated CO_2 concentrations are produced in the soil atmosphere as microbes decompose organic matter (derived from vegetation) and as plant roots respire. Percolating soil waters dissolve soil CO_2 and become acidified. Systematic isotopic fractionation occurs as carbon converts from $CO_{2(g)}$ to $CO_{2(aq)}$ to $HCO_3^-{}_{(aq)}$ to $CO_3^={}_{(aq)}$ (resulting in a net 10 to 11 per mil enrichment). Soil water $\delta^{13}C$ may be enriched further as carbonate bedrock [–3 to +4 per mil; J. D. Hudson, *Q. J. Geol. Soc. London* **33**, 637 (1977)] is dissolved enroute to underlying caves. Upon entering a cave passage of lowered CO_2 concentration, drip waters degas CO_2 and precipitate $CaCO_3$ as speleothems. Conditions of isotopic equilibrium are maintained between calcite and calcite-saturated fluids only when dissolved CO_2 is lost at a rate slow enough to maintain equilibrium between $HCO_3^-{}_{(aq)}$, $CO_3^={}_{(aq)}$, and $CO_{2(aq)}$ [C. H. Hendy, *Geochim. Cosmochim. Acta* **35**, 801 (1971)]; these conditions are best approximated in deep cave interiors where air circulation is minimal and temperature (which approximates mean annual temperature), CO_2 levels, and ~100% humidity remain stable throughout the year.
13. J. A. Dorale *et al.*, *Science* **258**, 1626 (1992); R. G.

Baker *et al.*, *Ecol. Monogr.* **66**, 203 (1996); R. G. Baker *et al.*, *Geology*, in press.
14. H. Zhu and R. G. Baker, *J. Paleolimnol.* **14**, 337 (1995).
15. E. Grüger, *Quat. Res.* **2**, 217 (1972).
16. At Pittsburg Basin (*15*), for example, the pollen sequence starts with a northern conifer assemblage (spruce, pine, fir, and larch), possibly representing the late-Illinoian glacial transition to the Sangamon interglacial. There follows a tripartite section in which the first and third zones are dominated by temperate hardwoods such as oak, hickory, elm, beech, walnut, and sweetgum and the middle zone by grasses, ragweed, and chenopods along with oak and other temperate hardwoods, a typical prairie-border or savanna assemblage. After an abrupt termination that probably represents a hiatus, the pollen is dominated by prairie-type taxa, leading up to a pine/birch zone and finally a spruce zone.
17. During the forest period from 55 to 25 ka, significant $\delta^{13}C$ excursions to more negative values culminate at ~52 and ~46 ka. These features may represent differences in the "openness" of the forest environment. Studies of modern closed-canopy forests have revealed that the increased recycling of plant-respired CO_2 [E. Medina, L. Sternberg, E. Cuevas, *Oecologia* **87**, 369 (1991)] and reduced light intensities [J. R. Ehleringer *et al.*, *ibid.* **70**, 520 (1986)] tend to shift plant tissues toward more negative $\delta^{13}C$ values when compared to a more open setting. One hallmark of the late-glacial boreal forests of the Midwest was their relative "openness," as suggested by their inclusion of shade-intolerant herbs like *Artemisia* and *Ambrosia* [D. C. Amundson and H. E. Wright Jr., *Ecol. Monogr.* **49**, 153 (1979)]. Thus, in addition to the physical controls of the forest canopy on understory $\delta^{13}C$ values, some opportunity for C_4 plant habitation may have also existed during the more "open" forest periods, reinforcing the trend toward less negative $\delta^{13}C$ values. Whether the collective consideration of these factors can be translated to a glacial-period forest dominated by conifers versus deciduous trees remains unclear.
18. W. Dansgaard, *Tellus* **16**, 438 (1964).
19. G. W. Moore and G. N. Sullivan, *Speleology*, (Zephyrus Press, Teaneck, NJ, ed. 2, 1978), p. 150.
20. This scenario neglects $\delta^{18}O$ variation of ocean water that occurred as ice volume fluctuated; including this factor would increase the temperature range estimate to more than 4°C.
21. I. Friedman, J. R. O'Neil, M. Fleischer, *U.S. Geol. Surv. Prof. Pap. 440-KK* (1977).
22. W. H. Johnson and L. R. Follmer, *Quat. Res.* **31**, 319 (1989).
23. B. B. Curry and L. R. Follmer, in *The Last Interglacial-Glacial Transition in North America*, P. U. Clark and P. D. Lea, Eds., *Geol. Soc. Am. Spec. Pap. 270* (1992), pp. 71–88.
24. D. S. Leigh, *Geol. Soc. Am. Bull.* **106**, 430 (1994).
25. ——— and J. C. Knox, *Quat. Res.* **39**, 282 (1993); B. B. Curry and M. J. Pavich, *ibid.* **46**, 19 (1996).
26. S. L. Forman *et al.*, *Palaeogeogr. Palaeoclimatol. Palaeoecol.* **93**, 71 (1992).
27. G. R. Whittecar and A. M. Davis, *Quat. Res.* **17**, 228 (1982).
28. E. A. Bettis III *et al.*, in *Iowa Geol. Surv. Bur. Guideb. Ser. No. 18* (1996), pp. 95–98; B. B. Curry, *Quat. Res.* **50**, 128 (1998).
29. D. G. Martinson *et al.*, *Quat. Res.* **27**, 1 (1987).
30. G. Bond *et al.*, *Nature* **365**, 143 (1993).
31. A. Baker, P. L. Smart, R. L. Edwards, *Geology* **23**, 309 (1995).
32. A. Berger and M. F. Loutre, *Quat. Sci. Rev.* **10**, 297 (1991).
33. We thank P. Hauck, G. Osburn, R. Young, and J. Morris for caving assistance and J. Hoff, H. Cheng, C. Borton, and R. McEwan for laboratory assistance. Reviews by H. E. Wright Jr. and D. A. Richards and discussions with E. C. Alexander Jr. helped improve the manuscript. Supported by NSF grants to R.L.E., E.I., and L.A.G. J.A.D. was supported by NSF-sponsored Research Training (to M. Davis) and Graduate Research Training (to M. Person) grants and a Geological Society of America student research grant.

16 July 1998; accepted 29 Octoer 1998

Oxygen Isotope Exchange Between Refractory Inclusion in Allende and Solar Nebula Gas

Hisayoshi Yurimoto,* Motoo Ito, Hiroshi Nagasawa

A calcium-aluminum–rich inclusion (CAI) from the Allende meteorite was analyzed and found to contain melilite crystals with extreme oxygen-isotope compositions (~5 percent oxygen-16 enrichment relative to terrestrial oxygen-16). Some of the melilite is also anomalously enriched in oxygen-16 compared with oxygen isotopes measured in other CAIs. The oxygen isotopic variation measured among the minerals (melilite, spinel, and fassaite) indicates that crystallization of the CAI started from oxygen-16–rich materials that were probably liquid droplets in the solar nebula, and oxygen isotope exchange with the surrounding oxygen-16–poor nebular gas progressed through the crystallization of the CAI. Additional oxygen isotope exchange also occurred during subsequent reheating events in the solar nebula.

Calcium-aluminum–rich inclusions (CAIs) are millimeter- to centimeter-sized objects composed of refractory minerals in chondrites and are widely believed to be the first solid particles formed in the solar nebula. The texture and composition of CAIs suggest that they were exposed to high temperatures, possibly during the infall phase that formed the sun and the solar nebula (*1*). Thus, CAIs were once molten or partially molten in the solar nebula. The crystallization sequence for a Ca-Al–rich silicate liquid is spinel, melilite, anorthite, and fassaite (*2*), and these minerals usually coexist in CAIs (*3*). Trace element distributions among the minerals is consistent with crystallization from a liquid state under assumed nebular conditions (*4*). If the constituent minerals were sequentially crystallized from such a liquid in an unchanging nebular environment, then the isotopic compositions of the minerals will be identical. However, oxygen isotope ratios are variable among the CAI minerals (*5, 6*).

In a three-isotope diagram, oxygen isotope ratios of CAI minerals, in general, are distributed along an ^{16}O component–enriched line called the carbonaceous chondrite anhydrous minerals (CCAM) line. The minerals at early- and late-crystallization stages are enriched in ^{16}O (spinel, $\delta^{17\text{ or }18}O_{SMOW}$ ~−40 per mil; fassaite, $\delta^{17\text{ or }18}O_{SMOW} = -20$ to −40 per mil) (*7*), whereas those at intermediate crystallization stages are less enriched in ^{16}O (melilite and anorthite, $\delta^{17\text{ or }18}O_{SMOW}$ ~0 per mil) (*6*). Although diffusive exchange after the crystallization of CAIs may explain the oxygen isotope heterogeneity (*8*), recent diffusion studies indicate that it is difficult to explain the observed O isotope distribution among CAI minerals by solid-gas diffusive exchange (*9*).

Recently a CAI containing ^{16}O-rich melilite in an ordinary chondrite was reported (*10*). The similarity of O isotopic composition between CAIs of carbonaceous and of ordinary chondrites suggests that they are genetically related and that CAI precursors were enriched in ^{16}O (*8*). On the basis of these measurements, the genetic link between the heterogeneous O isotope distribution among the constituent minerals and the igneous textures of CAIs has not been explained. Studies of the O isotope microdistribution within and among minerals may help to develop a model for the formation of the CAIs that explains their texture and O isotopic composition (*11*). Here we report on O isotopic evidence for the genesis of CAIs found in the Allende carbonaceous chondrite.

CAI 7R-19-1 was collected from the Allende CV3 chondrite, but the CAI is incomplete because of fragmentation during laboratory preparation. The CAI is round, and its diameter is estimated to be ~5 mm from the curvature of the CAI edge (Fig. 1). The CAI consists mainly of melilite (~70 volume %), fassaite (~15 volume %), and spinel (~10 volume %) grains. Minor mineral phases are hibonite and $CaTiO_3$ perovskite. Alteration products (anorthite; An_{99}, grossular) are present mainly along some grain boundaries between the major minerals. The melilite crystals have uniform or weakly zoned cores ($Åk_{13-20}$) and zoned rims ($Åk_{20-50}$) (Fig. 2). The large angular fassaite crystals usually have sector zoning and have a composition with a range of 11 to 16 weight % ($TiO_2 + Ti_2O_3$) and 17 to 22 weight % Al_2O_3. Small, rounded fassaite grains are observed within the melilite grains.

H. Yurimoto, Department of Earth and Planetary Sciences, Tokyo Institute of Technology, Ookayama, Meguro, Tokyo 152-8551, Japan. M. Ito and H. Nagasawa, Department of Chemistry, Gakushuin University, Mejiro, Toshima, Tokyo 171-8588, Japan.

*To whom correspondence should be addressed. E-mail: yuri@geo.titech.ac.jp